PACS 42.30.Wb, 95.85.Fm

S. E. Bankov, V. M. Chebotarev V. A. Cherepenin, A. V. Korjenevsky, A. V. Pestryakov, A. N. Vystavkin

V. A. Kotel'nikov Institute of Radioengineering and Electronics, RAS
125009, Mokhovaya Str. 11 bld. 7, Moscow, Russia
E-mail: vyst@hitech.cplire.ru

IMAGE PRODUCTION WITH SUB-DIFFRACTION RESOLUTION IN RADIO VISION DEVICES OF THE TERAHERTZ RANGE USING RECEIVING ARRAYS AND IMAGE SCANNING PROCEDURE

The earlier proposed method of image reconstruction with sub-diffraction resolution in radio vision devices (RVD) of the shortwave millimeter and Terahertz frequency range is analyzed. A brief description of the method including the algorithm is given. A computer simulation of the method including the results is described. The limitation of the method due to the noise effect is discussed.

Keywords: radio vision devices, receiving arrays, millimeter and Terahertz range, sub-diffraction resolution.

С. Е. Банков, В. М. Чеботарев, В. А.Черепенин, А. В. Корженевский, А. В. Пестряков, А. Н. Выставкин

ПОЛУЧЕНИЕ ИЗОБРАЖЕНИЙ С РАЗРЕШЕНИЕМ НИЖЕ ДИФРАКЦИОННОГО В УСТРОЙСТВАХ РАДИОВИДЕНИЯ ТЕРАГЕРЦЕВОГО ДИАПАЗОНА С ПРИМЕНЕНИЕМ МАТРИЧНЫХ ДЕТЕКТОРОВ И ПРОЦЕДУРЫ СКАНИРОВАНИЯ ИЗОБРАЖЕНИЯ

Анализируется предложенный ранее метод реконструкции изображения с разрешением ниже дифракционного в устройствах радиовидения (RVD) в коротковолновом и ТГц диапазонах. Дается краткое описание этого метода, включая алгоритм. Описывается компьютерное моделирование метода, включая результаты. Обсуждается ограничение метода из-за влияния шума.

Ключевые слова: устройства радиовидения, матричные детекторы, миллиметровый и ТГц диапазон, разрешение ниже дифракционного.

The method

The diffraction restriction in radio vision devices (RVD) of the short wave millimeter and Terahertz frequency range occurs when the RVD optical system Airy disc diameter d [1] is appreciably greater than the receiving element (RE) aperture $2R$: $d \gg 2R$. The receiving element is a combination of an input optical (quasioptical) concentrating component (horn, immersion lens or other) and a detector (for instance, nanobolometer) or a heterodyne mixer and some matching component between them, for instance, planar antenna plus a microstrip and coplanar lines. An RE example exploited at the laboratory of the authors work [2] is shown in Fig. 1.

The well known formula for the Airy disc diameter d [1] of RVD is

$$d = 2{,}44(\lambda/D)F, \qquad (1)$$

where λ is observed radiation wavelength, D is the diameter of the main mirror or the receiving antenna reflector and F is the effective focal distance of the Terahertz focusing optical (quasioptical) system of the radio vision device (RVD), for instance, telescope. Approximately 85% of the incident radiation beam power from a far-field zone point source is concentrated in the Airy disc.

ISSN 1818-7994. Вестник НГУ. Серия: Физика. 2010. Том 5, выпуск 4
Vestnik Novosibirsk State University. Series: Physics. 2010. Volume 5, issue 4

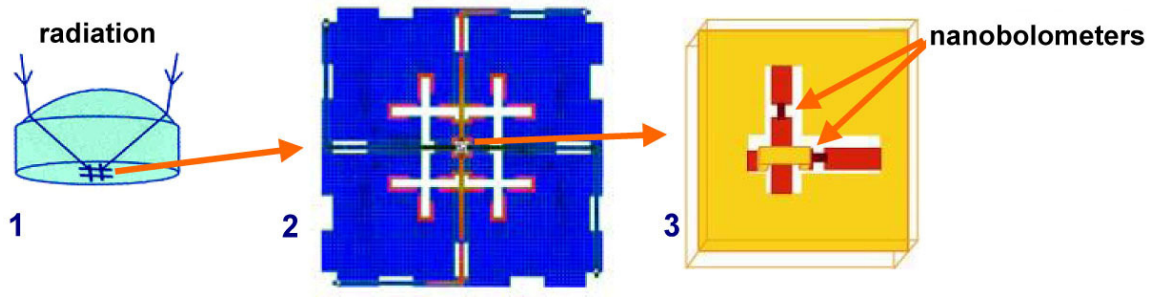

Fig.1: RE example: (1) Two-polarization crossed pair of double slot planar antennas installed in the focal plane of an immersion lens. (2) Configuration of the antennas. (3) Two-level intersection of a microstrip and coplanar lines with nanobolometers coupled into them, coplanar lines excited with antennas [2]

The described diffraction restriction occurs especially in the short wavelength millimeter and long wavelength portions of the THz range as in the transition part of the electromagnetic spectrum. The spatial resolution of observed images becomes worse in this case in comparison with the case when $d \le 2R$. A version of the method of image reconstruction with sub-diffraction resolution in RVDs of the short-wave millimeter and Terahertz frequency range was proposed in [3]. The method is based on image scanning using a two-dimensional RE array of RVDs when the RE array and the image move circularly relatively to each other (rotating or not rotating) in a common plane, with a small eccentricity between their centers (see an example in Fig. 2). The results of scanning are the signals $p_M(\theta)$ read out by detectors of the RE array. Each signal is proportional to the integral of the product of two functions. One function is the perfect image field distribution of the observed object received by the RVD without diffraction and other distortions. Let it be $f(x, y)$ and it is to be determined. The other function is the given RVD optical (quasioptical) transfer function comprising beams delivering the incident radiation to the RE array. Let it be

$$H_M(\theta, \vec{r}_s, \vec{r})$$

the RVD optical transfer function for the M^{th} receiving element, where

$$\vec{r} = (x, y)$$

are the coordinates in plane of image formation and

$$\vec{r}_s = (x_s, y_s)$$

are the coordinates of the array centre shift relatively to the image centre (the eccentricity). The second function takes into account the whole received radiation beam paths from the RVD input to each detector, including the effect of diffraction and reciprocal circular scanning of the array and the image. The image of the observed object itself (perfect with minimal distortions) can be found by solving the inverse ill-posed problem [4] determined by the above mentioned integral equations. Briefly, said equations, relating, for instance, to the scanning strategy presented in Fig. 2, have the following form:

$$p_M(\theta_j) = \int_{-R_I}^{R_I} \int_{-R_I}^{R_I} f(x,y) H_M[U(\theta_j, x_s, y_s, x, y), V(\theta_j, x_s, y_s, x, y)]dxdy, \qquad (2)$$

where U and V for two radiation polarizations (see Fig. 1) are

$$\left.\begin{aligned} U(\theta_j, x_s, y_s, x, y) &= (x - x_s) * \cos\theta_j + (y - y_s) * \sin\theta_j, \\ V(\theta_j, x_s, y_s, x, y) &= -(x - x_s) * \sin\theta_j + (y - y_s) * \cos\theta_j. \end{aligned}\right\} \qquad (3)$$

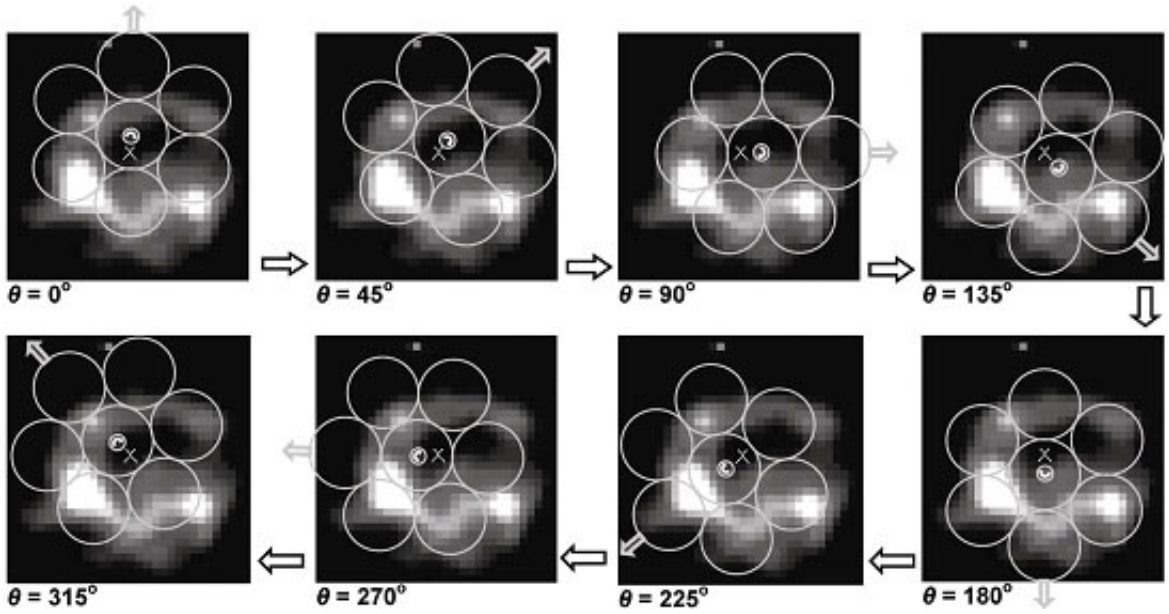

Fig. 2. Scanning strategy with image rotation relatively to the receiving array in their common plane using a K-mirror image rotator; 0^o … 315^o are the angle positions θ_j of the receiving array during the scanning with rotation relatively to the image. In this case the eccentricity is approximately $|r_s| \approx 0.3R$, where R is the radius of the RE

This procedure is repeated N_θ times. The amount N_θ of the angle positions θ_j is chosen so that to provide redundancy of the measured data. Since the functions

$$H_M(x, y)$$

are known, we have an integral equation for the function

$$f(x, y)$$

and can solve it by some computational methods. The solution can be found applying suitable equations and a regularization procedure [4]. The latter provides stability of the solution in the presence of the ill-posed right side of (1). See [3] for more details.

The computer simulation

We carried out the computer simulation of the method keeping in mind the Big Telescope Alt-azimuthal [5] for $\lambda \approx 1$ mm. The above concept and operation algorithm were used for this. The real image (Fig. 3,a) obtained in the short focus JCMT telescope [6] and used above for the scanning concept description was accepted as a perfect initial image for the simulation procedure. This procedure is illustrated in Fig. 3. The effect of diffraction in the long focus BTA telescope was simulated by means of multiplying the signal pixels taken from the initial image (Fig. 3,a) in the frames of each of the seven circles of the hexagonal "camomile" by the Airy function [1] and summing up the obtained products in the same frames. This procedure was repeated $N_\theta \geq 100$ times for the consecutive image to turn relatively to the receiving array again as in Fig. 2. One of the resulting sets of seven pixels (projections) at $\theta = 0$ constructed using the described procedure is represented in Fig. 3,b. The full obtained data set was used as imitation of really measured data and they were processed in accordance with the reconstruction algorithm described above. The result of the reconstruction is given in Fig. 3,c. The obtained reconstructed image looks acceptably similar to the initial one, keeping the 32×40 receiving element array of the JCMT in mind. Comparing the image in Fig. 3,b obtained as a single-step measurement and the reconstructed image in Fig. 3,c, one may conclude that the resolution is improved about ten times in this case. So, the fulfilled computer simulation estimation has shown that proposed method permits the resolution increasing in order of ten times

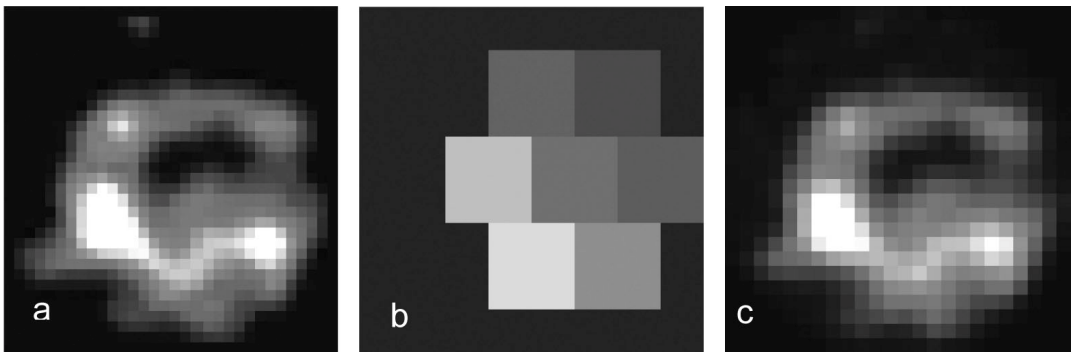

Fig. 3. Computer simulation of the image reconstruction in conformity with the BTA telescope: (a) the initial image taken from [6]; (b) one of results of the image "a" processed in accordance with the procedure described in the text, the eccentricity shift $|r_s| \approx 0.25R$ at θ = 0; (c) the result of solving equation (2) for $f(x, y)$ for a reconstruction array of 24×24 pixels

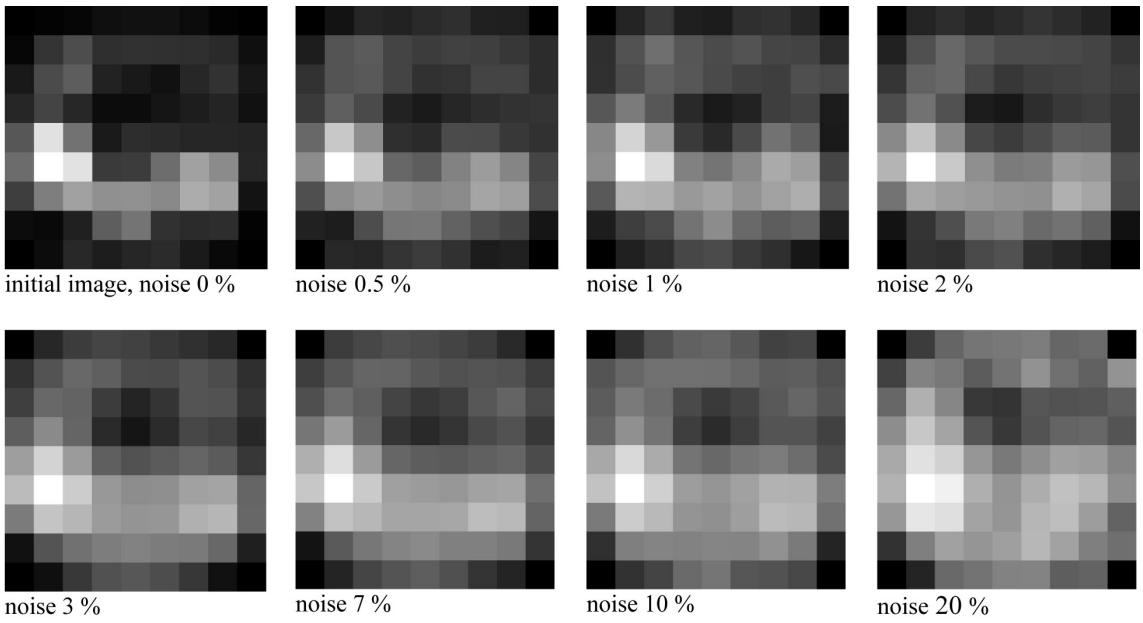

Fig. 4. Results of computer simulation of the noise effect on the reconstructed image

in comparison with the case of diffraction restriction.

Estimation of the noise effect

It is known [4] that the regularization procedure as part of the reconstruction algorithm is sensitive to the noise level in the receiving system. We carried out a computer simulation of the noise influence on the quality of reconstructed image. With this purpose we added various-level noise from a random-number generator to the signals $p_M(\theta)$ in (2). The initial image (Fig. 3,a) was transformed to 9×9 pixels to reduce the computer calculations. The noise intensity level is expressed in percents of the average image intensity. The computer simulation results are presented in Fig. 4. A noise level of 1 – 2 % can be accepted as maximally permissible from the viewpoint of image definition. This level may be achieved in radio vision devices, for instance, in space telescopes by means of application of very sensitive receiving detector

arrays [7] as well as via signal accumulation, increasing the observation time. The latter may have a sense for very important astrophysical objects.

References

1. *Longhurst R. S.*, "Geometrical and Physical Optics", 2nd Edition, Longmans, London (1968).

2. *Shitov S. V., Vystavkin A. N.*, Nucl. Instr. and Methods in Physics, Section A, V. 559, 2, pp. 503-505 (2006).

3. *Vystavkin A. N., Pestryakov A. V., Bankov S. E., Chebotarev V. M.*, Proc. SPIE, V. 7485, Paper 7485-24, pp. 1 – 8 (2009).

4. *Samarskij A. A., Vabistchevich P. N.*, Computational methods of inverse problems solving in mathematical physics (in Russian), Ed. 3, LKI Publishing House, Moscow (2009).

5. Special Astrophysical Observatory, http://www.sao.ru / Big Telescope Azimuthal.

6. *Greaves J. S., Holland W. S., Moriarty-Schieven G.* et al., The Astrophys. J., V. 506, 10, pp133–137 (1998).

7. *Cherepenin V. A., Vystavkin A. N., Kovalenko A. G. et al.*, this Symposium.

15.09.2010